China Ocean Eng., Vol. 30, No. 2, pp. 309 – 318

DOI 10.1007/s13344-016-0020-z, ISSN 0890-5487

Deep Sea AUV Navigation Using Multiple Acoustic Beacons*

JI Da-xiong (冀大雄)[a, b], SONG Wei (宋　伟)[a, 1],

ZHAO Hong-yu (赵宏宇)[b] and LIU Jian (刘　健)[b]

[a] *Ocean Collage, Zhejiang University, Zhoushan 316021, China*

[b] *State Key Laboratory of Robotics, Shenyang Institute of Automation, Chinese Academy of Sciences, Shenyang 110016, China*

(Received 28 March 2014; received revised form 30 July 2014; accepted 21 October 2014)

ABSTRACT

Navigation is a critical requirement for the operation of Autonomous Underwater Vehicles (AUVs). To estimate the vehicle position, we present an algorithm using an extended Kalman filter (EKF) to integrate dead-reckoning position with acoustic ranges from multiple beacons pre-deployed in the operating environment. Owing to high latency, variable sound speed multipath transmissions and unreliability in acoustic measurements, outlier recognition techniques are proposed as well. The navigation algorithm has been tested by the recorded data of deep sea AUV during field operations in a variety of environments. Our results show the improved performance over prior techniques based on position computation.

Key words: *deep sea AUV*; *acoustic navigation*; *range measurements*; *multiple beacons*; *outlier recognition*

1. Introduction

Reliable navigation is a critical ability for AUV, not only for the sake of safe operation and recovery of the AUV, but also for scientific surveys. AUVs are now being used for a variety of tasks, including oceanographic surveys, demining, and bathymetric data collection in marine and river environments. Accurate localization and navigation is essential to ensure the accuracy of the gathered data for the application. AUV navigation is a challenging problem due primarily to the rapid attenuation of higher frequency signals and the unstructured nature of the undersea environment. Above water, most autonomous systems rely on radio or spread-spectrum communications and global positioning. However, underwater, such signals propagate only short distances and acoustic-based sensors and communications perform better. Acoustic communications still suffer from many shortcomings such as narrow bandwidth, low data rate, high latency, variable sound speed, multipath transmissions and unreliability. In spite of these significant challenges, research in AUV navigation has exploded in the last ten years. Acoustic navigation system is still a popular method of underwater vehicle in deep sea. The field is in the midst of a paradigm shift from old technologies, such as long baseline (LBL), which require pre-deployed and localized infrastructure, toward dynamic system approaches that allow for rapid deployment and flexibility with minimal infrastructure. Another system "ultra short baseline (USBL)" is employed to track and locate the underwater vehicle (Ji and Zheng,

---

* This work was financially supported by the National Natural Science Foundation of China (Grant No. 51309215).

1 Corresponding author. E-mail: weisong@zju.edu.cn

2013). However, acoustic navigation algorithm of deep sea AUVs is pretty challenging because it is a bit difficult to design an effective online processing procedure for travel time measurements which may be affected by noise, drop outs and outliers. Past reviews on this topic includes Stutters *et al*. (2008), Kinsey *et al*. (2006), Paull *et al*. (2014). In fact the predominant source of the spurious measurements is the presence of multiple acoustic propagation paths between source and receiver. The AUV must make decisions regarding the quality of the data without the aid of a human operator. Of course the reliability of the decision should be high in order to keep AUV safe and high navigation accuracy. A major consideration in acoustic navigation is the treatment of outliers. Methods to account for outliers in LBL systems include hypothesis grids (Bingham and Seering, 2006) and graph partitioning (Olson *et al*., 2006). Generally, range measurements can fall into one of three categories: direct path (DP), multipath (MP), or outlier (OL). The quality of range data is dependent on the location within the survey area (Ji and Liu, 2010). In (Bingham and Seering, 2006), a hypothesis grid is built to represent the belief that future measurements from a particular cell will be in a particular category (i.e., DP, MP, and OL). In graph partitioning, outliers are rejected using spectral analysis. A set of measurements is represented as a graph and the graph partitioning algorithm is applied to identify sets of consistent measurement (Olson *et al*., 2006). Another consideration is the time difference of arrival (TDOA) of the acoustic responses of the network (Bishop *et al*., 2008; McPhail and Pebody, 2009). The change in vehicle pose between the initial interrogation request and all of the subsequent replies must be explicitly handled. This is often done with a delayed state EKF. Each range difference measurement between two receivers constrains the target to an annulus (in 2-D) or a sphere (in 3-D). Annuluses are intersected to find the location of the target. However, when the data are corrupted by noise, there is not necessarily an intersection point.

Our AUV is a deep ocean vehicle of 6000 meters, which was developed at Shenyang Institute of Automation. As part of its sensor suite, a custom multiple beacons navigation system was equipped on the AUV. To estimate the vehicle position, we present an algorithm that uses an extended Kalman filter (EKF) to integrate dead-reckoning position with acoustic ranges from multiple beacons pre-deployed in the operating environment. Most importantly, an effective method for processing raw measurements is adopted in the filter on account to that measurements process is a prerequisite for the EKF in the presence of spurious measurements. The algorithm was successfully applied to “Qianlong 1”AUV in the trial. The structure of this paper is as follows. In Section 2, the problem of multiple beacons navigation of AUVs is described. Section 3 discusses the central problem of measurements process. Section 4 presents experimental results obtained with the algorithm and compares its performance with the conventional navigation algorithm based on EKF but without outlier rejection. Finally, Section 5discusses the results and future research directions.

2. Multiple-Beacon Navigation

Multiple-beacon navigation refers to an underwater position referencing system employing an array of acoustic beacons, as shown in Fig. 1. Beacon separations for most vehicle applications are typical from hundreds of meters to a few kilometers. These beacons are always calibrated before AUV operation.

Owing to the latency of acoustic updates, state estimators are implemented where the DR sensors provide the predictions and then acoustic measurements provide the updates. There is one prevalent filtering approach for position estimation when processing range measurements (Ji *et al*., 2009). This is to update the predicted position with fix computation based on more than three range measurements. In this case, the position is usually computed by depth and not less than three distances of beacons and used to correct position estimates by a Kalman filter (KF). While the navigation approach we presented here is to directly update the predicted position by range measurements. To be more specific, the depth and each range measurement or travel time are directly regarded as an observing value in the measurement equation in the extended Kalman filter (EKF). That also is, the presented method does not explicitly compute a fix, but provides a position estimate which is a weighted combination of dead reckoning results and absolute measurements, and consequently leading to a smoother track because a successive set of travel time is only utilized to partly correct the predicted position instead of totally updating in the first approach. Therefore the second approach was designed for deep sea navigation.

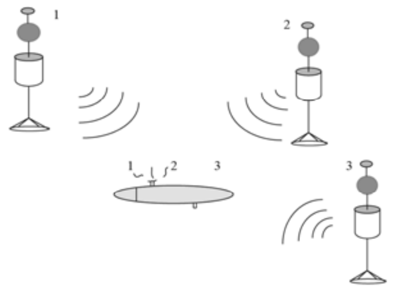

Fig. 1. Multiple beacon position.

2.1 State Model of the EKF

Since the depth can be obtained by depth sensor on the AUV, obviously we only need to establish the local horizontal frame of geography other than three-dimensional frame. According to the conventional custom, the *x*-axis points east, and the *y*–axis points north. The AUV position in this frame is denoted by (x, y) and accordingly the coordinates of beacon i (i = 1, 2, ...) are denoted by(x_i, y_i). The measured travel time between the vehicle and the beacon is denoted by t_i and the associated distances is denoted by d_i. The round trip distance is computed from the round trip travel time by the approximate relationship: $d_i=c(t_i-\tau_i)$, where c is the average speed of sound and τ_i is the turn around time of beacon i.

The position prediction stage of the EKF is given as below. This state model is identical with the classical dead-reckon navigation:

$$\begin{bmatrix} x \\ y \end{bmatrix}_k = \begin{bmatrix} x \\ y \end{bmatrix}_{k-1} + \mathrm{d}t \begin{bmatrix} v_x \\ v_y \end{bmatrix}_{k-1} + w_{k-1} \tag{1}$$

where dt is the sample time, w_{k-1} is the process noise, and v_x and v_y are the east speed and north speed respectively. They are the well-known function involving yaw, pitch, roll and speed vector in the vehicle frame. These angles and speed are gained from relevant sensors on the AUV. For example, if heading is available from a compass and velocity is available from a Doppler velocity log (DVL), (v_x,

v_y) is achieved by using the following kinematic equations:

$$\begin{cases} v_x = v\cos\psi + u\sin\psi \\ v_y = -v\sin\psi + u\cos\psi \end{cases} \tag{2}$$

where u and v are the body frame forward and starboard velocities. In this model, it is assumed that roll and pitch are zero and that depth is measured accurately with a depth sensor. It is worth noticing that an inertial system is an alternative of electronic compass that aims to improve upon the dead-reckon pose estimation by integrating measurements from accelerometers and gyroscopes. However, one problem with inertial system is that they drift over time. One common approach, for example, is to maintain the drift as part of the state space (Miller *et al*., 2010).

2.2 Observation Model of the EKF

As far as the filters mentioned above are concerned, they are easily distinguished from their own observation models. In the first approach, the fix is a set of measurements of each state and thus its observation model is linear. While in the second approach, the travel time is a single measurement of the whole states and its observation model is clearly nonlinear. In fact the second approach provides the filter process with specific advantages. To begin with, this approach is more suitable to deal with independent measurement. The travel time from each beacon are measured and output at different time because of different ranges from each beacon to the vehicle and consequently the travel times is a set of independent measurements. Therefore these measurements can be filtered independently rather than not processed until more than three periods of travel times come up for fix computation. It is obvious that the presented approach contribute more to position estimation than the first one in terms of real time and filtering rate. Another important point is that the presented approach can take account of the vehicle movement during the period of travel time. This is because the observation model in the EKF describes a real time model of round trip from pinging moment to receiving moment. By contrast, the fix computation in the KF always assumes that the vehicle is stationary between the ping and the reception and naturally leading to an error in the vehicle position from the fix computation. Fortunately, the presented approach can address this issue with its spontaneous advantage. As shown in Fig. 2 where AUV starts pinging at point $(x_\mathrm{p}, y_\mathrm{p}, z_\mathrm{p})$ and receives the acoustic signal from one transponder at point $(x_\mathrm{r}, y_\mathrm{r}, z_\mathrm{r})$, and the acoustic travel range equals the range between pinging location and the transponder plus the range between receiving location and the transponder. Obviously the receiving point coordination is the sum of pinging point coordination and displacement $(x_\mathrm{d}, y_\mathrm{d}, z_\mathrm{d})$.

Besides the travel time between pinging and receiving, every transponder has its own delay time τ_i which must be considered into the observation equation. Thus the observation equation for the overall travel time can be expressed as a function of the position at the ping and at the reception of the return:

$$t_i = \frac{1}{c}\sqrt{(x_\mathrm{p}-x_i)^2+(y_\mathrm{p}-y_i)^2+(z_\mathrm{p}-z_i)^2} + \frac{1}{c}\sqrt{(x_\mathrm{r}-x_i)^2+(y_\mathrm{r}-y_i)^2+(z_\mathrm{r}-z_i)^2} + \tau_i \tag{3}$$

$$x_\mathrm{p} = x_\mathrm{r} - x_\mathrm{d}(t_i),\ y_\mathrm{p} = y_\mathrm{r} - y_\mathrm{d}(t_i),\ z_\mathrm{p} = z_\mathrm{r} - z_\mathrm{d}(t_i)\,,$$

where i = 1, 2, 3, …, p and r denotes the ping and reception, $x_{\mathrm{d}}(t_i)$, $y_{\mathrm{d}}(t_i)$ and $z_{\mathrm{d}}(t_i)$ denote the vehicle displacement in three axes between the ping and reception. It is noticeable that the vehicle movement can be obtained from dead-reckon.

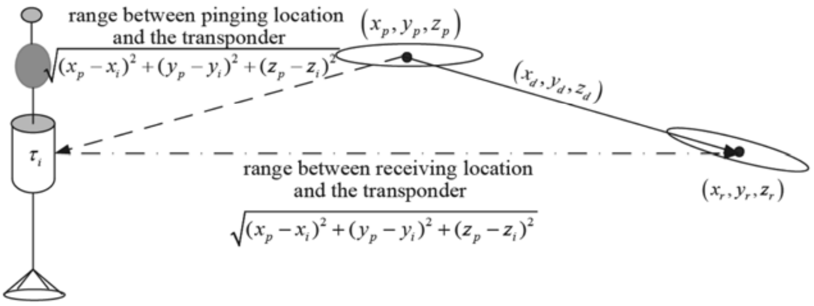

Fig. 2. Sketch diagram of observation equation.

3. Outlier Recognition

It is generally assumed that measurement errors consist of zero-mean additive noise. However, in fact the acoustic travel times involve a large amount of outliers, especially in the severe condition. This may not only produce a false initial position, but also result in a bad track. To avoid these unsatisfied effects, the navigation algorithm of AUV should be designed to account for outliers. It is general knowledge that both false initial states and false measurements are the keys to acoustic navigation of AUV.

For initial position confirmation, a novel method is proposed here referring to multiple-object tracking algorithm. The confirmation of initial position is much the same as initial object tracks in terms of initial trajectory estimation. It is common sense that an unreal initial position must be beyond basic rules, while the real abides these rules. Thus this proposed method is employed for initial position confirmation, involving the processing of a sequence of measurements received during consecutive range measurements. The sequence of measurements represents the input to a time-window containing N measurements. When the number of detections contained in the window reaches a specified value, a successful track initiation is obtained; otherwise the window is moved one scan towards the right, i.e. for increasing time. Suppose that $\boldsymbol{r}_j$, j = 1, 2, ..., N is the position of AUV from N consecutive fix computation and T is the period of acoustic pinging. The proposed method initiates a track if any M (<N) measurements from these N fix computations satisfy the following requirements:

(1) The measured or estimated velocity is greater than a minimum value, $v_{\min}$ and less than a maximum value, $v_{\max}$.

(2) The measured or estimated acceleration is less than a maximum value, $a_{\max}$. If there is more than one return, the one with the minimum acceleration is used to form the new track. Mathematically, the two rules can be expressed as

$$v_{\min}\cdot T \le \left|\boldsymbol{r}_j - \boldsymbol{r}_{j-1}\right| \le v_{\max}\cdot T\ ; \tag{4}$$

$$\left|(\boldsymbol{r}_{j+1}-\boldsymbol{r}_j)\text{-}(\boldsymbol{r}_j-\boldsymbol{r}_{j-1})\right| \le a_{\max}\cdot T^2 . \tag{5}$$

As far as the outlier rejection is concerned, there are two traditional different ways in which outlier rejection could be performed: in the time domain (travel time rejection) or in the spatial domain (fix rejection). Since it takes only one bad travel time value to result in an erroneous position, fix rejection has the potential to discard too much information. Therefore, temporal outlier rejection is desirable because erroneous travel times can be rejected individually. The short time accuracy of dead reckoning is acceptable and can predict where the vehicle should be. Rejection of outliers could take advantage of this ability. The position uncertainty is mainly due to two factors: initial position and bad measurements. Furthermore, during the dead reckoning process, validation region for each of travel time is defined by transforming the position uncertainty to the travel time domain. The EKF can directly perform this transformation. When the vehicle dead reckons, the position is predicted using the state equation (1). The associated error covariance is also predicted by:

$$P_{k/k-1}=F_{k-1}P_{k-1}F_{k-1}+Q_{k-1}, \tag{6}$$

where F_k is the Jacobian matrix of the state vector with respect to the speed and orientation, and Q_k is the covariance matrix of the state noise in Eq. (1). After propagation of the position error, the uncertainty in position is transformed into uncertainty in the predicted travel time using observation equation. Outliers are judged by the data association gate algorithm. Predicting state $\boldsymbol{x}_k$ can be assumed as Gauss distribution and its mean is $\hat{\boldsymbol{x}}_{k/k-1}$. Since predicting state is conditioned by all history measurements, the distribution of predicting state can be regarded as approximate summary associated with history information. Thus this summary can be described below

$$p\left[\boldsymbol{x}_k\middle|\boldsymbol{t}_{k-1}\right]=\boldsymbol{N}\left[\boldsymbol{x}_k;\hat{\boldsymbol{x}}_{k|k-1},P_{k|k-1}\right], \tag{7}$$

where $\boldsymbol{t}_{k-1}$ means all the measurements up to k–1, the right part of the equation above means probability density function (pdf) of Gauss distribution where x_k is the variable, $\hat{\boldsymbol{x}}_{k|k-1}$ is the mean and $P_{k|k-1}$ is the covariance matrix. Under the assumption as shown in Eq. (7), we can define an ellipse area as shown in Fig. 3 where the measurements can be confirmed as below:

$$d_{i,k}^2=\left[t_{i,k}-\hat{t}_{k/k-1}\right]^{\mathrm{T}}S_k^{-1}\left[t_{i,k}-\hat{t}_{k/k-1}\right]\le\gamma, i=1,2,\dots,N_0 \tag{8}$$

with

$$S_k=H_kP_{k/k-1}H_k^t+\sigma_t^2, \tag{9}$$

where γ is the threshold, $d_{i,k}^2$ means the statistical distance which conforms to x^2 distribution, N_0 is the number of all the measurements at time k, j means the order number of measurements, H is the travel time Jacobian and σ_t denotes the standard error. Fig. 3 illustrates a confirmation area for measurements. We can see that the statistical distances of measurements $t_{i,k}(i=1,2,4)$ all meet the requirement in Eq. (8), but the statistical distance of $t_{i,k}$ is bigger than γ and thus $t_{i,k}$ does not fall into the confirmation area.

When a new travel time arrives, its normalized innovation squared is compared with the threshold γ. Then a validated measurement can be used to correct the predicted position after confirmed by Eq. (8). The threshold γ is important for the navigation method, because it determines how many measurements we can use in the algorithm. How to choose a reasonable threshold γ? Generally, we assume that the noise of measurement obeys Gaussian distribution with standard error σ_t and the measurement error is usually defined as two times σ_t under probability of 0.9954 for measurement sensors. We can deduce that variable s^2/σ_t^2 obeys χ^2 distribution where s means the standard error of the sample. Since the dimension of travel time measurements is single, we have from $\chi^2(1)$ distribution

$$p\left(s^2/\sigma_t^2 \le 4\right) = 0.9545\,. \tag{10}$$

Considering d_k^2 is the estimate of s^2/σ_t^2 with certain error, we increase the probability to 0.998 to enlarge the confirmed area. That is

$$p\left(d_k^2 \le \gamma\right) = 0.998\,. \tag{11}$$

From $\chi^2(1)$ distribution, we can obtain γ =9.21.

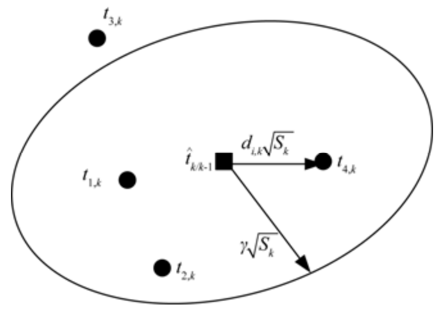

Fig. 3. Confirming area for the measurements.

4. Experimental Results

The proposed algorithm has run in “Qianlong 1”AUV, as shown in Fig. 4. The experiments were carried out in March and Jun. separately in the year 2013. There were two totally different acoustic conditions as shown in Fig. 3 and Fig. 4, respectively. In the experiments, the period T of acoustic pinging is 24 s, $v_{\max}$ and $v_{\min}$ are 4 m/s and 0 m/s respectively, $a_{\max}$ is 0.5 m/s^2, and γ is 9.21. The heading sensor is TCM5, and the speed sensor is Doppler Velocity Log. There were four acoustic beacons to be deployed at the sea bottom. The presented algorithm is based on EKF with outlier recognition. We test the presented algorithms to compare with the conventional navigation algorithm which is also based on EKF but without outlier rejection by the record data of two voyages in the trial. In order to compare with the error of two navigation algorithms, we give the discrete track by fix computation that directly uses range measurements to calculate the vehicle’s position. Fig. 5 and Fig. 7 show the vehicle tracks estimated by the two navigation algorithms in voyage 1 and voyage 2 respectively and Fig. 6 and Fig. 8 show the error comparison of two navigation algorithms (without outlier rejection vs. with outlier rejection).

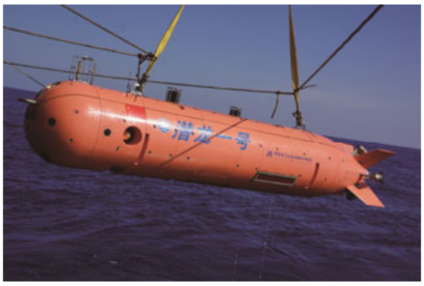

Fig. 4. “Qianlong 1” AUV.

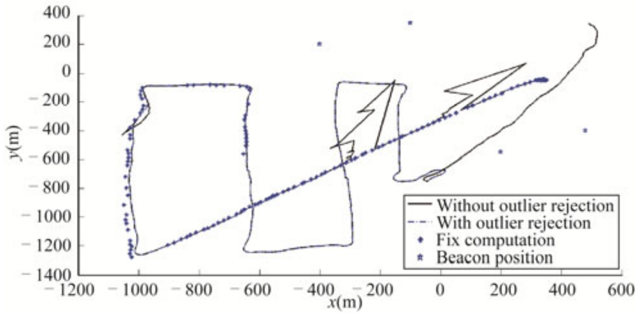

Fig. 5. Tracks comparison of two navigation algorithms (without outlier rejection vs. with outlier rejection) in voyage 1.

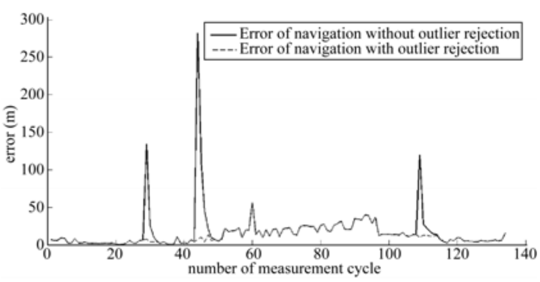

Fig. 6. Error comparison of two navigation algorithms(without outlier rejection vs. with outlier rejection) for Fig. 5.

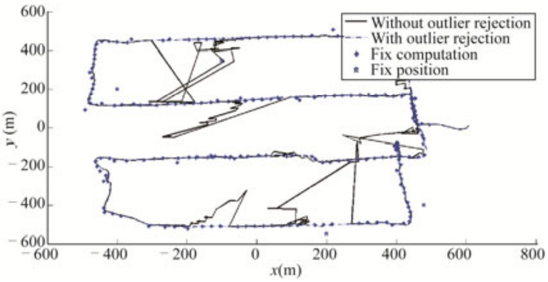

Fig. 7. Tracks comparison of two navigation algorithms (without outlier rejection vs. with outlier rejection) in bad acoustic condition in voyage 2.

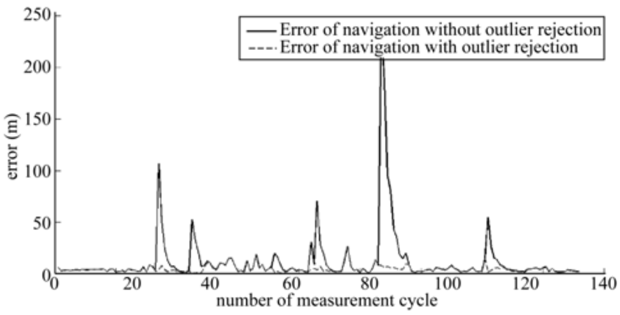

Fig. 8. Error comparison of two navigation algorithms (without outlier rejection vs. with outlier rejection) for Fig. 8 errors caused by the two algorithms.

We emphasize that all the two algorithms employ the initial position confirmation method in Eqs. (4) and (5). It can be noted in Figs. 5 and 7 that the two algorithms ensure the correct initial position using the proposed method. This experiment proves that the proposed approach is valid on initial position confirmation. Besides that, what is most manifest from the charts is that the two methods mentioned above demonstrate different performances in position estimation. Firstly, we can directly see from both Fig. 5 and Fig. 7 that the track estimated by the presented algorithm is much smoother than that by the conventional algorithm. Evidently, in addition, the error of the presented algorithm is much smaller than that of the conventional algorithm in Fig. 6 and Fig. 8. Moreover, it is obvious that the acoustic condition is good in Fig. 5 as there are few jumps in the track estimated by the conventional algorithm, whereas it is bad in Fig. 4 as there are a few jumps. This demonstrates that the presented algorithm has a nice performance even in bad condition of measurements. The plots indicate that the travel time measurements which passed the validation test can indeed correct the vehicle position, while the false measurements are dropped out to avoid disturbing the estimates. In contrast, the track estimated by the conventional algorithm produces more significant jumps in worse condition. This trend is illustrated clearly in the two voyages. The reason for these jumps is primarily that outliers from raw measurements have not been rejected and as a result the estimates are contaminated. Consequently the conventional method is easily subjected to measurement quality which depends on the acoustic condition. In fact, as these jumps deviate from actual track very far, the track estimated by the conventional algorithm is unacceptable for the vehicle navigation.

The error statistics are given in Tables 1 and 2. The mean in the tables is obtained by absolute value of position error. We can see that the error mean of the presented algorithm is very small compared with that of the conventional algorithm. More precisely, for the error mean of the presented algorithm, the mean is 10.7 m and the standard error is 9.2 m in Table 1 and the mean is 4.2 m and the standard error 3.5 m in Table 2. The standard error is less than the mean. Whereas, for the conventional algorithm, the error mean is at least 1.5 times that of the presented algorithm. Moreover, the standard error is much larger than the mean itself. This is caused by jumps in the track. These results demonstrate that the presented algorithm is superior to the conventional algorithm not only in accuracy but also in uniformity. Furthermore, we can notice that the mean and standard error of the presented algorithm in Table 2 is smaller than that in Table 1. This is owing to the cause that there are more valid measurements in voyage 2 than that in voyage 1 to be utilized by the presented algorithm.

Table 1 Error statistics in voyage 1

	Mean (m)	Standard error (m)
Conventional algorithm	16.3	31.5
Presented algorithm	10.7	9.2

Table 2 Error statistics in voyage 1

	Mean (m)	Standard error (m)
Conventional algorithm	11.6	26.9
Presented algorithm	4.2	3.5

It is common sense that the fix computation algorithm uses at least 3 travel times to calculate the position. The position outliers can be rejected by Eq. (8) on a subset of the measurements, but all these travel times may be discarded together with the position outliers during each measurement circle. This procedure will lead to too much waste on valuable measurements for the operation of acoustic beacons is very hard in the sea trial (Ji *et al*., 2010). Thus it is required to utilize as many valid returns as possible during a cycle to completely correct the error of the vehicle position estimates. As it happens, the presented algorithm can process an independent travel time in every circle. However, this kind of procession may inevitably induce the nonlinearity of observation equation that may partially, not globally correct the estimates in each measurement update. Nevertheless this situation can be compensated by many measurements update.

5. Conclusion

The proposed approach on initial position confirmation is validated by the experiment. Moreover, the presented extended Kalman filter with proposed outlier recognition has most satisfactory performance compared with the conventionally extended Kalman filter and fix computation. It should be noticeable that another source of error in fix computation is that the navigation sensor noise of the vehicle is not taken into account. In the near future, it would be desirable to implement a more theoretically advanced technique for position estimation. The nice approach would be to employ M-estimate algorithm for this purpose (Đurović and Kovačević,, 1999). The regression problem on noise in EKF can be solved robustly using the M-estimate algorithm. It can become adaptive estimation of the unknown a priori state and noise statistics simultaneously with the system states. This ability will make the vehicle track more accurate.

References

Bingham, B. and Seering, W., 2006. Hypothesis grids: Improving long baseline navigation for autonomous underwater vehicles, *IEEE J. Oceanic Eng.*, **31**(1): 209–218.

Bishop, A., Fidan, B., Anderson, B., Dogancay, K. and Pathirana, P., 2008. Optimal range-difference-based localization considering geometrical constraints, *IEEE J. Oceanic Eng*., **33**(3): 289–301.

Đurović, Ž. and Kovačević, B., 1999. Robust estimation with unknown noise statistics, *IEEE Transactions on Automatic Control*, **44**(6): 1292−1296.

Ji, D. X. and Liu, J., 2010. Ray theory application in long baseline system, *China Ocean Eng*., **24**(1): 199−206.

Ji, D. X. and Zheng, R., 2013. Acoustic theory application in ultra short baseline system for tracking AUV, *Marine Geodesy*, **36**(4): 428–435.

Ji, D. X., Li, Y. P. and Liu, J., 2010. Seafloor transponder calibration using improved perpendiculars intersection, *Appl. Ocean Res.*, **32**(3): 261−266.

Ji, D. X., Liu, J. and Zhou, B., 2009. The position estimate method of AUV with low cost navigation system, *Chinese Journal of Scientific Instrument*, **30**(1): 35−38. (in Chinese)

Kinsey, J. C., Eustice, R. M. and Whitcomb, L. L., 2006. A survey of underwater vehicle navigation: Recent advances and new challenges, *Proc. Conf. Manoeuvering Control Marine Craft*, 1–12.

McPhail, S. D. and Pebody, M., 2009. Range-only positioning of a deep-diving autonomous underwater vehicle from a surface ship, *IEEE J. Oceanic Eng.*, **34**(4): 669−677.

Miller, P. A., Farrell, J. A., Zhao, Y. and Djapic, V., 2010. Autonomous underwater vehicle navigation, *IEEE J. Oceanic Eng.*, **35**(3): 663–678.

Olson, E., Leonard, J. J. and Teller, S., 2006. Robust range-only beacon localization, *IEEE J. Oceanic Eng*., **31**(4): 949–958.

Paull, L., Saeedi, S., Seto, M. and Li, H., 2014. AUV Navigation and Localization: A Review, *IEEE J. Oceanic Eng.*, **39**(1): 131−149.

Stutters, L., Liu, H., Tiltman, C. and Brown, D. J., 2008. Navigation technologies for autonomous underwater vehicles, *IEEE Trans. Syst. Man Cybern. C*: *Appl. Rev*., **38**(4): 581–589.